

# Radiative corrections to neutral pion-pair production

N. Kaiser

Physik-Department T39, Technische Universität München, D-85747 Garching, Germany

## Abstract

We calculate the one-photon loop radiative corrections to the neutral pion-pair photoproduction process  $\pi^- \gamma \rightarrow \pi^- \pi^0 \pi^0$ . At leading order this reaction is governed by the chiral pion-pion interaction. Since the chiral  $\pi^+ \pi^- \rightarrow \pi^0 \pi^0$  contact-vertex depends only on the final-state invariant-mass it factors out of all photon-loop diagrams. We give analytical expressions for the multiplicative correction factor  $R \sim \alpha/2\pi$  arising from eight classes of contributing one-photon loop diagrams. An electromagnetic counterterm has to be included in order to cancel the ultraviolet divergences generated by the photon-loops. Infrared finiteness of the virtual radiative corrections is achieved (in the standard way) by including soft photon radiation below an energy cut-off  $\lambda$ . The radiative corrections to the total cross section vary between +2% and -2% for center-of-mass energies from threshold up to  $7m_\pi$ . The finite part of the electromagnetic counterterm gives an additional constant contribution of about 1%, however with a large uncertainty.

PACS: 12.20.Ds, 12.39.Fe, 13.40.Ks

## 1 Introduction and summary

The pions ( $\pi^+$ ,  $\pi^0$ ,  $\pi^-$ ) are the Goldstone bosons of spontaneous chiral symmetry breaking in QCD. Their strong interaction dynamics at low energies can therefore be calculated systematically (and accurately) with chiral perturbation theory in form of a loop expansion based on an effective chiral Lagrangian. The very accurate two-loop predictions [1] for the S-wave  $\pi\pi$ -scattering lengths,  $a_0 = (0.220 \pm 0.005)m_\pi^{-1}$  and  $a_2 = (-0.044 \pm 0.001)m_\pi^{-1}$ , have been confirmed experimentally by analyzing the  $\pi\pi$  final-state interaction effects occurring in various (rare) charged kaon decay modes [2, 3, 4]. Electromagnetic processes with pions offer further possibilities to test chiral perturbation theory. For example, pion Compton scattering  $\pi^- \gamma \rightarrow \pi^- \gamma$  allows one to extract the electric and magnetic polarizabilities ( $\alpha_\pi$  and  $\beta_\pi$ ) of the charged pion. Chiral perturbation theory at two-loop order gives for the dominant pion polarizability difference the firm prediction  $\alpha_\pi - \beta_\pi = (5.7 \pm 1.0) \cdot 10^{-4} \text{ fm}^3$  [5]. It is however in conflict with the existing experimental results from Serpukhov  $\alpha_\pi - \beta_\pi = (15.6 \pm 7.8) \cdot 10^{-4} \text{ fm}^3$  [6] and MAMI  $\alpha_\pi - \beta_\pi = (11.6 \pm 3.4) \cdot 10^{-4} \text{ fm}^3$  [7] which amount to values more than twice as large. Certainly, these existing experimental determinations of  $\alpha_\pi - \beta_\pi$  raise doubts about their correctness since they violate the chiral low-energy theorem notably by a factor 2. It is worth to note that a recent dispersive analysis [8] of the Belle data for  $\gamma\gamma \rightarrow \pi^+\pi^-$  gives the fit value  $\alpha_\pi - \beta_\pi = 4.7 \cdot 10^{-4} \text{ fm}^3$ , compatible with chiral perturbation theory.

In that contradictory situation it is promising that the ongoing COMPASS experiment [9] at CERN aims at remeasuring the pion polarizabilities,  $\alpha_\pi$  and  $\beta_\pi$ , with high statistics using the Primakoff effect. The scattering of high-energy negative pions in the Coulomb-field of a heavy nucleus (of charge  $Z$ ) gives access to cross sections for  $\pi^- \gamma$  reactions through the equivalent photon method [10]. The consistent theoretical framework to extract the pion polarizabilities from the measured cross sections for (low-energy) pion Compton scattering  $\pi^- \gamma \rightarrow \pi^- \gamma$  or the primary pion-nucleus bremsstrahlung process  $\pi^- Z \rightarrow \pi^- Z \gamma$  has been described (in one-loop approximation) in refs.[11, 12]. It has been stressed that at the same

order as the polarizability difference  $\alpha_\pi - \beta_\pi$  there exists a further (partly compensating) pion-structure effect in form of a unique pion-loop correction (interpretable as photon scattering off the "pion-cloud around the pion"). In addition to these strong interaction effects, the QED radiative corrections to real and virtual pion Compton scattering  $\pi^- \gamma^{(*)} \rightarrow \pi^- \gamma$  have been calculated in refs.[12, 13]. The relative smallness of the pion-structure effects in low-energy pion Compton scattering [11] makes it necessary to include such higher order electromagnetic corrections. The COMPASS experiment is set up to detect simultaneously various (multi-particle) hadronic final-states which are produced in the Primakoff scattering of high-energy pions. The neutral pion production channel  $\pi^- \gamma \rightarrow \pi^- \pi^0$  serves as a test of the QCD chiral anomaly by measuring the  $\gamma 3\pi$  coupling constant  $F_{\gamma 3\pi} = e/(4\pi^2 f_\pi^3) = 9.72 \text{ GeV}^{-3}$ . For the two-body process  $\pi^- \gamma \rightarrow \pi^- \pi^0$  the one-loop [11, 14] and two-loop corrections [15] of chiral perturbation theory as well as QED radiative corrections [16] have already been worked out.

The  $\pi^- \gamma$  reaction with three charged pions in the final-state is used in the energy range above 1 GeV to study the spectroscopy of non-strange meson resonances [17] and to search for so-called exotic meson resonances [18]. The very high statistics of the COMPASS experiment allows it to continue the event rates with three pions in the final-state even downward to the threshold. The (differential) cross sections for the  $\pi^- \gamma \rightarrow 3\pi$  reactions in the low-energy region offer new possibilities to test the strong interaction dynamics of the pions as predicted by chiral perturbation theory. In a recent work [19] the production amplitudes for  $\pi^- \gamma \rightarrow \pi^- \pi^0 \pi^0$  and  $\pi^- \gamma \rightarrow \pi^+ \pi^- \pi^-$  have been calculated analytically at one-loop order in chiral perturbation theory. It has been found that the next-to-leading order corrections from chiral loops and counterterms enhance sizeably (by a factor 1.5 – 1.8) the total cross section for neutral pion-pair production  $\pi^- \gamma \rightarrow \pi^- \pi^0 \pi^0$ . By contrast the total cross section for charged pion-pair production  $\pi^- \gamma \rightarrow \pi^+ \pi^- \pi^-$  remains almost unchanged in comparison to its tree-level result. This different behavior can be understood from the varying influence of the chiral corrections on the pion-pion final-state interaction ( $\pi^+ \pi^- \rightarrow \pi^0 \pi^0$  versus  $\pi^- \pi^- \rightarrow \pi^- \pi^-$ ).

The purpose of the present paper is to further improve the theoretical description of the  $\pi^- \gamma \rightarrow 3\pi$  reactions by considering the corresponding QED radiative corrections. We restrict ourselves here to the simpler case of neutral pion-pair production  $\pi^- \gamma \rightarrow \pi^- \pi^0 \pi^0$ , for which the number of contributing one-photon loop diagrams is limited to about a dozen. Another fortunate circumstance is that the (leading-order) chiral  $\pi^+ \pi^- \rightarrow \pi^0 \pi^0$  contact-vertex factors out of all photon-loop diagrams and therefore the radiative corrections to  $\pi^- \gamma \rightarrow \pi^- \pi^0 \pi^0$  can be represented simply by a multiplicative correction factor  $R \sim \alpha/2\pi$ . Infrared finiteness of these virtual radiative corrections is achieved (in the standard way) by including soft photon radiation below an energy cut-off  $\lambda$ . Taking  $\lambda = 5 \text{ MeV}$ , we find that the radiative corrections to the total cross section for  $\pi^- \gamma \rightarrow \pi^- \pi^0 \pi^0$  vary between +2% and –2% for center-of-mass energies from threshold up to  $7m_\pi$ . An electromagnetic counterterm (necessary in order to cancel all ultraviolet divergences generated by the photon-loops) gives an additional constant contribution of about 1%, however with a large uncertainty. The radiative corrections to the charged pion-pair production process  $\pi^- \gamma \rightarrow \pi^+ \pi^- \pi^-$  can be roughly estimated to be a factor 2–4 times larger, arguing that in this case twice as many charged pions are involved in virtual photon-loops and soft photon bremsstrahlung.

## 2 Evaluation of one-photon loop diagrams

In this section we calculate analytically the radiative corrections to the neutral pion-pair photoproduction process:

$$\pi^-(p_1) + \gamma(k, \epsilon) \rightarrow \pi^-(p_2) + \pi^0(q_1) + \pi^0(q_2), \quad (1)$$

as they arise from one-photon loop diagrams at order  $\alpha$ . For a concise presentation of our analytical results it is convenient to introduce the following dimensionless Mandelstam variables:

$$s = (p_1 + k)^2/m_\pi^2, \quad t = (p_1 - p_2)^2/m_\pi^2, \quad u = (p_2 - k)^2/m_\pi^2, \quad (2)$$

with  $m_\pi = 139.570$  MeV the charged pion mass. In this (adapted) notation  $\sqrt{s}m_\pi$  is the total center-of-mass energy of the process. We will also use frequently the linear combination:

$$\Sigma = s + t + u - 2 = (q_1 + q_2)^2/m_\pi^2, \quad (3)$$

related to the squared invariant mass of the produced neutral pion-pair. In the physical region the following inequalities hold:  $s > (1 + 2\sqrt{r_0})^2$ ,  $t < 0$ ,  $u < 0$ <sup>1</sup> and  $4r_0 < \Sigma < (\sqrt{s} - 1)^2$  where  $r_0 = (m_{\pi^0}/m_\pi)^2 = 0.93526$  denotes the squared ratio between the neutral pion mass  $m_{\pi^0} = 134.977$  MeV and the charged pion mass  $m_\pi$ .

Let us recall the dynamical description of the process  $\pi^- \gamma \rightarrow \pi^- \pi^0 \pi^0$  at low energies [11, 19]. When choosing for the (transversal) real photon  $\gamma(k, \epsilon)$  the Coulomb-gauge in the center-of-mass frame, the conditions  $\epsilon \cdot p_1 = \epsilon \cdot k = 0$  imply that all diagrams for which the photon couples to the in-coming pion  $\pi^-(p_1)$  vanish identically. Furthermore, in the convenient parametrization of the special-unitary matrix-field  $U = \sqrt{1 - \vec{\pi}^2/f_\pi^2} + i\vec{\tau} \cdot \vec{\pi}/f_\pi$  no  $\gamma 4\pi$  and  $2\gamma 4\pi$  contact-vertices exist (at leading order). Under these assumptions one is left with one single  $u$ -channel pole diagram in which the chiral  $\pi^+ \pi^- \rightarrow \pi^0 \pi^0$  contact-vertex is followed by a photon-pion coupling proportional to  $\epsilon \cdot p_2$ .

The virtual radiative corrections to  $\pi^- \gamma \rightarrow \pi^- \pi^0 \pi^0$  are obtained by dressing this tree diagram with a photon-loop in all possible ways (see Figs.1-4). A fortunate circumstance is that the (leading order) chiral  $\pi^+ \pi^- \rightarrow \pi^0 \pi^0$  transition amplitude  $[(q_1 + q_2)^2 - m_{\pi^0}^2]/f_\pi^2$  depends only on the  $\pi^0 \pi^0$  invariant mass and thus factors out of all photon-loop diagrams. The Coulomb-gauge ( $\epsilon \cdot p_1 = \epsilon \cdot k = 0$ ) leaves the scalar product  $\epsilon \cdot p_2$  as the only possible coupling term for the external real photon. As a consequence of these features the radiative corrections due to photon-loops can be represented simply by a multiplicative correction factor. Its real part which is only of relevance is denoted by  $R(s, t, u)$ . We use dimensional regularization to treat both ultraviolet and infrared divergences (where the latter are caused by the masslessness of the photon). Divergent pieces of one-loop integrals show up in form of the composite constant:

$$\xi = \frac{1}{d-4} + \frac{1}{2}(\gamma_E - \ln 4\pi) + \ln \frac{m_\pi}{\mu}, \quad (4)$$

containing a simple pole at  $d = 4$  and  $\mu$  is an arbitrary mass scale. Ultraviolet (UV) and infrared (IR) divergences are distinguished by the feature of whether the condition for convergence of the  $d$ -dimensional integral is  $d < 4$  or  $d > 4$ . We discriminate them in the notation by putting appropriate subscripts, i.e.  $\xi_{UV}$  and  $\xi_{IR}$ . In order to simplify all calculations we employ the Feynman gauge, where the photon propagator is directly proportional to the Minkowski metric tensor  $g_{\mu\nu}$ . We can now enumerate the analytical expressions for  $R(s, t, u)$  as they emerge from the eight classes of contributing one-photon loop diagrams.

The two diagrams of class (I) shown in Fig.1 introduce the wavefunction renormalization factor  $Z_2 - 1$  of the pion [12]:

$$R^{(I)} = \frac{\alpha}{\pi}(\xi_{IR} - \xi_{UV}). \quad (5)$$

---

<sup>1</sup>The inequality  $u < 1$  follows immediately from the definition of  $u$ . In order to derive the sharper upper bound  $u < 0$ , one uses the relation for  $u$  written in eq.(21) and inserts  $y_{\max} = 1$  and  $\omega_{\max} = (s + 1 - 4r_0)/2\sqrt{s}$ . In the end the condition  $r_0 > 1/4$  turns out to be crucial for  $u$  to take on only negative values.

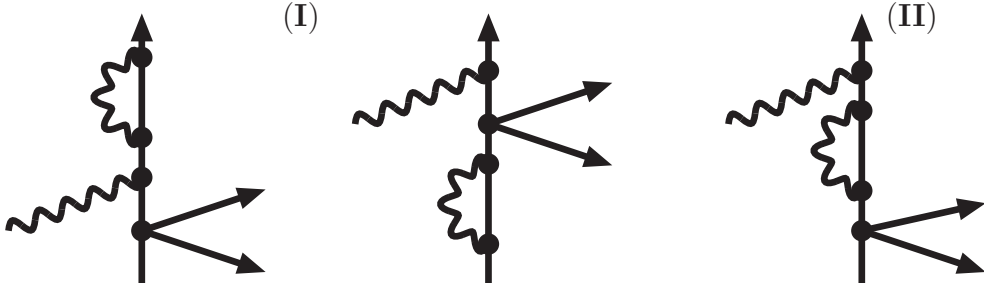


Figure 1: One-photon loop diagrams (I) and (II) for neutral pion-pair production  $\pi^- \gamma \rightarrow \pi^- \pi^0 \pi^0$ . Arrows indicate out-going pions.

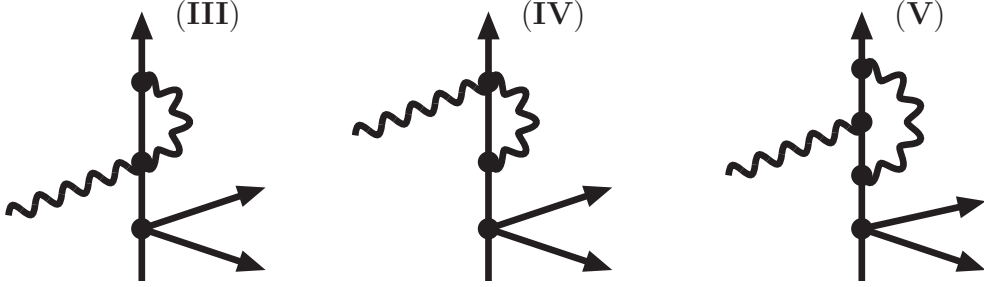


Figure 2: One-photon loop diagrams (III), (IV) and (V).

Diagram (II) involves the once-subtracted (off-shell) selfenergy of the pion and leads to the result:

$$R^{(\text{II})} = \frac{\alpha}{\pi} \left[ -\xi_{UV} + 1 - \frac{u+1}{2u} \ln(1-u) \right]. \quad (6)$$

Diagram (III) shown in Fig.2 gives rise a constant vertex correction:

$$R^{(\text{III})} = \frac{\alpha}{8\pi} (6\xi_{UV} - 7), \quad (7)$$

while diagrams (IV) and (V) generate  $u$ -dependent vertex corrections:

$$R^{(\text{IV})} = \frac{\alpha}{8\pi} \left[ 6\xi_{UV} - 6 - \frac{1}{u} + \frac{u-1}{u^2} (3u+1) \ln(1-u) \right], \quad (8)$$

$$R^{(\text{V})} = \frac{\alpha}{8\pi} \left[ -4\xi_{UV} + 5 + \frac{1}{u} + \frac{u^2 + 6u + 1}{u^2} \ln(1-u) \right]. \quad (9)$$

It is astonishing that the last four contributions  $R^{(\text{II})} + R^{(\text{III})} + R^{(\text{IV})} + R^{(\text{V})} = 0$  sum to zero.

The reducible  $u$ -channel pole diagram (VI) shown in Fig.3 includes a photonic vertex correction around the  $2\pi^0$  emission vertex. One finds for its contribution to the (real)  $R$ -factor the following result:

$$R^{(\text{VI})} = \frac{\alpha}{2\pi} \left\{ -\xi_{UV} + 1 + \frac{1-u}{2u} \ln(1-u) + \sqrt{\frac{\Sigma-4}{\Sigma}} \ln \frac{\sqrt{\Sigma-4} + \sqrt{\Sigma}}{2} \right. \\ \left. + \left( s+t + \frac{u-7}{2} \right) \int_0^1 dx \frac{\ln|x^{-1} + \Sigma(x-1)| - \ln(1-u)}{1 + (u-1)x + \Sigma x(x-1)} \right\}. \quad (10)$$

The integrand of the principal-value integral  $\int_0^1 dx$  has simple poles at  $x_{\pm} = [\Sigma + 1 - u \pm \sqrt{(\Sigma + 1 - u)^2 - 4\Sigma}]/2\Sigma$ , but in the physical region  $u < 0$ ,  $\Sigma > 4r_0$  only the pole at  $x_-$  lies

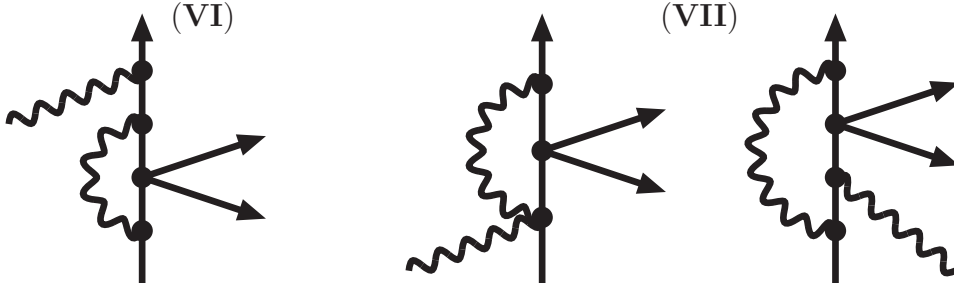


Figure 3: One-photon loop diagrams (VI) and (VII).

inside the unit-interval  $0 < x < 1$ . Due to this property an accurate numerical treatment of the principal-value integral in eq.(10) (in combination with further three-body phase space integrations, see eq.(20)) is easily manageable. We have also checked the Feynman parameter representation of the last loop integral in eq.(10) against its dispersion relation representation:

$$\int_0^1 dx \frac{\ln |x^{-1} + \Sigma(x-1)| - \ln(1-u)}{1 + (u-1)x + \Sigma x(x-1)} = \int_4^\infty \frac{dx}{x-\Sigma} \frac{2}{\sqrt{(x+1-u)^2 - 4x}} \times \ln \frac{\sqrt{x}(x-u-3) + \sqrt{(x-4)[(x+1-u)^2 - 4x]}}{2(1-u)}, \quad (11)$$

where the imaginary part on the right hand side has been calculated via the Cutkosky cutting rule. The analytical continuation of the last logarithmic term in the first line of eq.(10) for  $0 < \Sigma < 4$  is  $\sqrt{4/\Sigma - 1} \arcsin(\sqrt{\Sigma}/2)$ .

In the sum  $R^{(I)} + R^{(VI)}$  obtained so far the ultraviolet divergences  $\xi_{UV}$  do not cancel and the remaining classes of diagrams (VII) and (VIII) are actually ultraviolet convergent. In a non-renormalizable effective field theory like chiral perturbation theory such a behavior of the radiative corrections is generic. In order to eliminate all ultraviolet divergences from photon-loops additional electromagnetic counterterms have to be introduced [20]. The black square in the right tree diagram of Fig.4 symbolizes the pertinent electromagnetic counterterm for  $\pi^+\pi^- \rightarrow \pi^0\pi^0$  scattering. It gives rise to the following constant contribution to the  $R$ -factor:

$$R^{(ct)} = \frac{3\alpha}{2\pi} (\xi_{UV} + \bar{k}), \quad (12)$$

where  $\bar{k}$  denotes the finite part of the electromagnetic counterterm which remains after canceling the ultraviolet divergence  $\xi_{UV}$ . A numerical estimate of  $\bar{k}$  will be given in section 4. For the sake of completeness we quote the expression for the on-shell  $\pi^+(q_+) + \pi^-(q_-) \rightarrow \pi^0(q_1) + \pi^0(q_2)$  scattering amplitude with inclusion of radiative corrections [20]:

$$T_{+-,00} = \frac{m_\pi^2}{f_\pi^2} (\Sigma - r_0) \left\{ 1 + \frac{\alpha}{2\pi} \left[ 2(\xi_{IR} - \xi_{UV}) + 3(\xi_{UV} + \bar{k}) - \xi_{UV} + 1 + \sqrt{\frac{\Sigma-4}{\Sigma}} \left( \ln \frac{\sqrt{\Sigma-4} + \sqrt{\Sigma}}{2} - \frac{i\pi}{2} \theta(\Sigma-4) \right) + (\Sigma-2) \int_4^\infty \frac{dx}{x-\Sigma-i0^+} \frac{2\xi_{IR} + \ln(x-4)}{\sqrt{x^2-4x}} \right] \right\}, \quad (13)$$

where  $\Sigma = (q_1 + q_2)^2/m_\pi^2$  and  $f_\pi = 92.4 \text{ MeV}$  denotes the pion decay constant. In the order given the terms in the square bracket correspond to the pion wavefunction renormalization

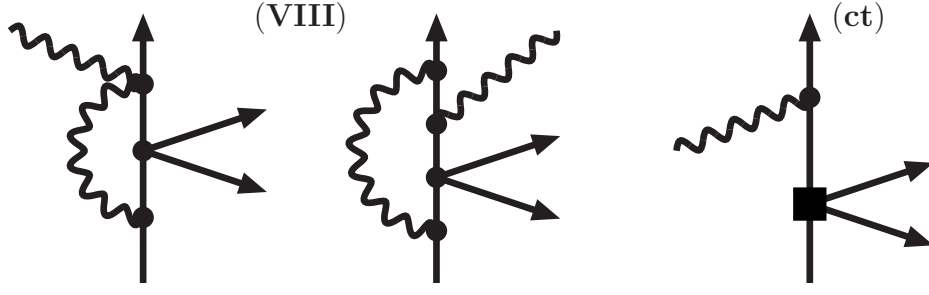


Figure 4: One-photon loop diagrams (VIII). The black square in the right tree diagram (ct) symbolizes the electromagnetic counterterm for  $\pi^+\pi^- \rightarrow \pi^0\pi^0$  scattering.

factor  $Z_2 - 1$ , the electromagnetic counterterm, and the one-photon exchange contribution. Note that we have used the (concise) spectral function representation for the infrared divergent (scalar) loop integral involving one photon and two pion propagators. If an infinitesimal photon mass  $m_\gamma$  is introduced as an (alternative) infrared regulator the infrared divergence  $\xi_{IR}$  is to be identified with the logarithm  $\ln(m_\pi/m_\gamma)$ .

Next, we come to the irreducible  $s$ -channel diagrams of class (VII) shown in Fig. 3. Since the contribution from the left diagram (involving the two-photon contact-vertex) gets (partly) canceled by a term from the right diagram it is advantageous to specify only their total contribution to the  $R$ -factor. After reducing the loop integrals with four propagators one obtains the following result:

$$\begin{aligned}
 R^{(VII)} = & \frac{\alpha}{2\pi}(u-1) \left\{ \frac{D(t) - D(\Sigma)}{2(\Sigma - t)} + \int_0^1 dx \frac{1 - 2x + 2x^2}{1 - tx(1-x)} \right. \\
 & \left. \times \frac{\ln|x^{-1} + \Sigma(x-1)| - \ln(s-1)}{1 + (s-1)x + \Sigma x(x-1)} \right\}. \quad (14)
 \end{aligned}$$

Note that the last denominator has no poles in the physical region, since  $s-1 + \Sigma(x-1) > s-1 - \Sigma > s-1 - (\sqrt{s}-1)^2 = 2(\sqrt{s}-1) > 0$ . By taking the absolute magnitude of the arguments of logarithms one gets directly a suitable representation of the only relevant real part. It is a fortunate circumstance that the Feynman-parameter representation of loop functions leads to expressions which can be handled easily numerically in the physical region.

Finally, we come to the irreducible  $u$ -channel diagrams of class (VIII) shown in Fig. 4. The contribution from the left diagram gets completely absorbed by a term from the right diagram. The resulting contribution to the (real)  $R$ -factor includes an infrared divergent term with a non-trivial  $t$ -dependence and after putting all pieces together it reads:

$$\begin{aligned}
 R^{(VIII)} = & \frac{\alpha}{2\pi} \left\{ \frac{1-u}{2} \left[ \frac{D(t) - D(\Sigma)}{\Sigma - t} - \frac{1}{u} \ln(1-u) \right] \right. \\
 & + \int_0^1 dx \frac{1 + 4x^2 - tx(1+x)}{1 - tx(1-x)} \frac{\ln|x^{-1} + \Sigma(x-1)| - \ln(1-u)}{1 + (u-1)x + \Sigma x(x-1)} \\
 & + \frac{t-2}{\sqrt{t^2-4t}} \left[ 4(\xi_{IR} + \ln(1-u)) \ln \frac{\sqrt{4-t} + \sqrt{-t}}{2} + \text{Li}_2(w) \right. \\
 & \left. - \text{Li}_2(1-w) + \frac{1}{2} \ln^2 w - \frac{1}{2} \ln^2(1-w) + \text{Li}_2(h_-) - \text{Li}_2(h_+) \right] \\
 & \left. + (2-t) \int_0^1 dx \frac{\ln|1 + \Sigma x(x-1)|}{1 - tx(1-x)} \right\}, \quad (15)
 \end{aligned}$$

with the abbreviations

$$w = \frac{1}{2} \left( 1 - \sqrt{\frac{-t}{4-t}} \right), \quad h_{\pm} = \frac{1}{2} \left( t \pm \sqrt{t^2 - 4t} \right). \quad (16)$$

One observes that the term proportional to  $D(t) - D(\Sigma)$  drops out in the sum  $R^{(\text{VII})} + R^{(\text{VIII})}$  and therefore we do not need to specify it.  $\text{Li}_2(w) = \sum_{n=1}^{\infty} n^{-2} w^n = w \int_1^{\infty} dx [x(x-w)]^{-1} \ln x$  denotes the conventional dilogarithmic function. Several of the results derived in section 3 of ref.[13] have been useful in order to obtain the expression for  $R^{(\text{VIII})}$  written in eq.(15).

### 3 Infrared finiteness

In the next step we have to consider the infrared divergent terms proportional to  $\xi_{IR}$  present in eqs.(5,15). At the level of the measurable cross section these get eliminated by contributions from (undetected) soft photon bremsstrahlung. In its final effect, the (single) soft photon radiation off the in- or out-going  $\pi^-$  multiplies the tree-level differential cross section for  $\pi^- \gamma \rightarrow \pi^- \pi^0 \pi^0$  by a (universal) factor [12, 13]:

$$\delta_{\text{soft}} = 2R_{\text{soft}} = \alpha \mu^{4-d} \int_{|\vec{l}| < \lambda} \frac{d^{d-1}l}{(2\pi)^{d-2} l_0} \left\{ \frac{2p_1 \cdot p_2}{p_1 \cdot l p_2 \cdot l} - \frac{m_{\pi}^2}{(p_1 \cdot l)^2} - \frac{m_{\pi}^2}{(p_2 \cdot l)^2} \right\}, \quad (17)$$

which depends on a small energy cut-off  $\lambda$ . Working out this momentum space integral by the method of dimensional regularization (with  $d > 4$ ) one finds the following contribution from soft photon emission to the  $R$ -factor:

$$\begin{aligned} R_{\text{soft}}^{(\text{cm})} &= \frac{\alpha}{4\pi} \left\{ 4 \left[ 1 + \frac{2t-4}{\sqrt{t^2-4t}} \ln \frac{\sqrt{4-t} + \sqrt{-t}}{2} \right] \left( \ln \frac{m_{\pi}}{2\lambda} - \xi_{IR} \right) \right. \\ &\quad + \frac{s+1}{s-1} \ln s + \frac{2\omega}{\sqrt{\omega^2-1}} \ln (\omega + \sqrt{\omega^2-1}) + (t-2) \\ &\quad \left. \times \int_0^1 dx \frac{s+1-\Sigma x}{[1-tx(1-x)]\sqrt{W}} \ln \frac{s+1-\Sigma x + \sqrt{W}}{s+1-\Sigma x - \sqrt{W}} \right\}, \quad (18) \end{aligned}$$

with the abbreviation  $W = (s+1-\Sigma x)^2 - 4s[1-tx(1-x)]$ . In order to simplify the last term in eq.(18) we have made use of the relation  $\Sigma = s+1-2\omega\sqrt{s}$ , where  $\omega$  denotes the center-of-mass energy of the out-going negative pion  $\pi^-(p_2)$  divided by  $m_{\pi}$ . Note that the terms beyond those proportional to  $\ln(m_{\pi}/2\lambda) - \xi_{IR}$  are specific for the evaluation of the soft photon correction factor  $R_{\text{soft}}$  in the center-of-mass frame with  $\lambda$  an infrared cut-off therein.

In order to present a concrete example we have evaluated the complete radiative correction factor  $R$  at the threshold in the isospin limit:  $s_{\text{th}} = 9$ ,  $t_{\text{th}} = -4/3$ ,  $u_{\text{th}} = -5/3$ ,  $\Sigma_{\text{th}} = 4$ ,  $\omega_{\text{th}} = 1$ . In this case one gets numerically:

$$R_{\text{th}} = \frac{\alpha}{2\pi} \left\{ 11.093 + 3\bar{k} + \left( 2 - \frac{5}{2} \ln 3 \right) \ln \frac{m_{\pi}}{2\lambda} - 0.725 \right\}, \quad (19)$$

where the terms in the curly bracket correspond in the order written to virtual photon-loops, the electromagnetic counterterm, the universal soft photon contribution, and the soft photon contribution specific for imposing an infrared cut-off via  $|\vec{l}| < \lambda$  in the center-of-mass frame.

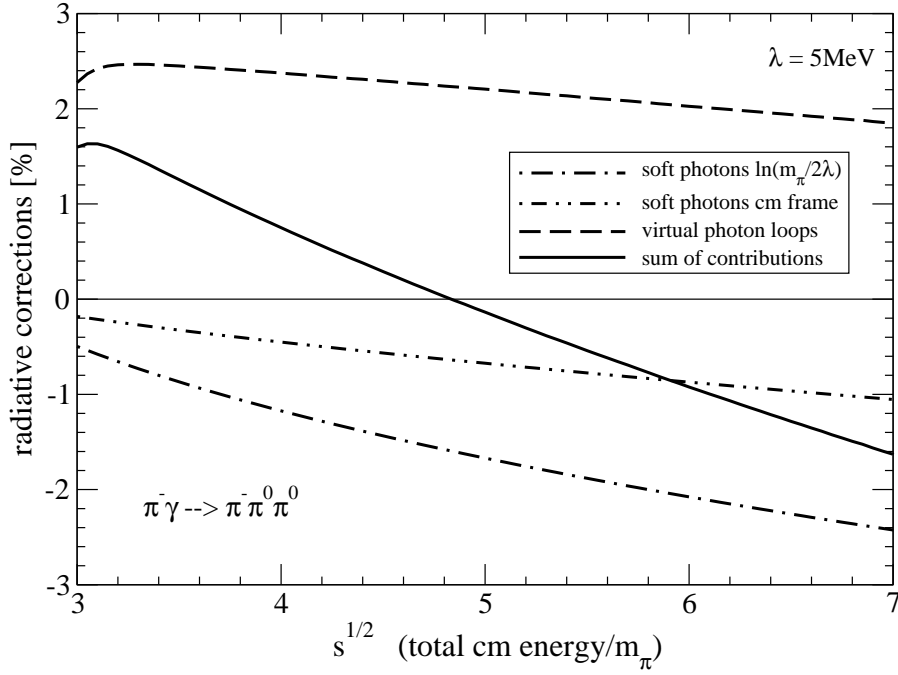


Figure 5: Radiative corrections to the total cross section for neutral pion-pair photoproduction  $\pi^- \gamma \rightarrow \pi^- \pi^0 \pi^0$  as a function of the center-of-mass energy  $\sqrt{s} m_\pi$ . The infrared cut-off for soft photon emission has been set to the value  $\lambda = 5$  MeV.

## 4 Results: radiative corrections to cross sections

After inclusion of radiative corrections the total cross section for neutral pion-pair production  $\pi^- \gamma \rightarrow \pi^- \pi^0 \pi^0$  depends also on the infrared cut-off  $\lambda$  for undetected soft photons. We multiply the squared tree-level amplitude by  $1 + 2R(s, t, u, \lambda)$  and integrate over the three-pion phase space. Applying the usual flux and symmetry factors the total cross section reads:

$$\begin{aligned} \sigma_{\text{tot}}(s, \lambda) &= \frac{\alpha m_\pi^2}{32\pi^2 f_\pi^4 (s-1)} \int_1^{\omega_{\text{max}}} d\omega (\omega^2 - 1)^{3/2} \sqrt{\frac{\Sigma - 4r_0}{\Sigma}} \\ &\quad \times \int_{-1}^1 dy (1 - y^2) \left( \frac{\Sigma - r_0}{u - 1} \right)^2 [1 + 2R(s, t, u, \lambda)], \end{aligned} \quad (20)$$

with  $\omega_{\text{max}} = (s + 1 - 4r_0)/2\sqrt{s}$  the endpoint energy of the out-going  $\pi^-$  divided by  $m_\pi$ . Using the relations  $\Sigma = s + t + u - 2 = s + 1 - 2\omega\sqrt{s}$  and:

$$u = 1 + \frac{1-s}{\sqrt{s}} (\omega - y\sqrt{\omega^2 - 1}), \quad t = 2 - (s+1) \frac{\omega}{\sqrt{s}} + \frac{1-s}{\sqrt{s}} y\sqrt{\omega^2 - 1}, \quad (21)$$

valid in the center-of-mass frame the whole integrand in eq.(20) becomes a function of  $\omega$  and the directional cosine  $y$ .

Fig. 5 shows in percent the radiative corrections to the total cross section for neutral pion-pair production  $\pi^- \gamma \rightarrow \pi^- \pi^0 \pi^0$  as a function of the center-of-mass energy  $\sqrt{s} m_\pi$ . The dashed-dotted and dashed curves display the separate contributions from soft photon bremsstrahlung and virtual photon-loops. In each case the radiative correction is calculated as the ratio of the shift in  $\sigma_{\text{tot}}(s, \lambda)$  induces by the respective  $R$ -factor divided by the tree-level cross section. As in ref.[12] the infrared cut-off  $\lambda$  for undetected soft photons has been set to  $\lambda = 5$  MeV, a value which seems appropriate for the COMPASS experiment. The full line in Fig. 5 shows the complete radiative corrections. One observes an almost linear decrease which ranges from



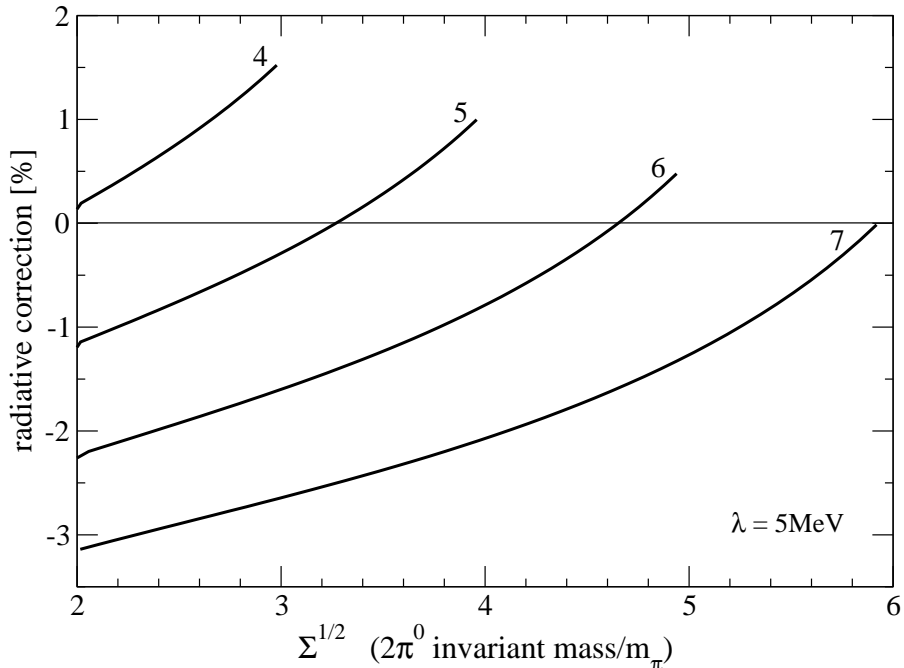


Figure 6: Radiative corrections to the  $\pi^0\pi^0$  mass spectra for neutral pion-pair production  $\pi^-\gamma \rightarrow \pi^-\pi^0\pi^0$  as a function of the  $\pi^0\pi^0$  invariant mass  $\sqrt{\Sigma}m_\pi$ . The numbers on the curves correspond to  $\sqrt{s}$ .

+1.6% at threshold to  $-1.6\%$  at the center-of-mass energy  $\sqrt{s}m_\pi = 7m_\pi$ . An interesting feature is that the positive radiative corrections from the virtual photon-loops get gradually reduced and turned into negative values by the soft photon contributions.

The finite part of the electromagnetic counterterm  $\bar{k}$  shifts the radiative corrections (displayed by the full curve in Fig. 5) by a constant amount of  $3\alpha\bar{k}/\pi = 0.7\% \cdot \bar{k}$ . In order to give an estimate for  $\bar{k}$  we exploit the elaborate result of ref.[21] for the pionium decay amplitude  $(a_0 - a_2)m_\pi + \varepsilon$ . Guided by eq.(13) we identify  $(\alpha/2\pi)(3\bar{k} + 1)$  with the ratio  $\varepsilon^{\text{elm}}/(a_0 - a_2)$ , where  $\varepsilon^{\text{elm}}$  is the electromagnetic correction to the pionium decay amplitude. Subtracting from  $\varepsilon = (6.1 \pm 1.6) \cdot 10^{-3}$  the contribution  $4.8 \cdot 10^{-3}$  due to the (charged and neutral) pion mass difference (see eqs.(4.28,4.29) in ref.[21]) one gets  $\varepsilon^{\text{elm}} = (1.3 \pm 1.6) \cdot 10^{-3}$ . Together with the leading order expression for the  $\pi\pi$ -scattering length difference  $a_0 - a_2 = 9m_\pi/(32\pi f_\pi^2) = 0.204m_\pi^{-1}$  one arrives at the estimate  $\bar{k} = 1.5 \pm 2.2$  for the electromagnetic counterterm. Its central value implies a constant shift of the radiative corrections to  $\pi^-\gamma \rightarrow \pi^-\pi^0\pi^0$  by about 1.0%. The large errorbar of  $\bar{k} = 1.5 \pm 2.2$  introduces at the same time a wide errorband to the full curve in Fig. 5. Still an allowed option is to neglect to electromagnetic counterterm, setting  $\bar{k} = 0$ .

Finally, we consider radiative corrections to more exclusive observables. An obvious candidate is the  $\pi^0\pi^0$  mass spectrum  $d\sigma/dm_{00}$  with  $m_{00} = \sqrt{\Sigma}m_\pi$  the  $\pi^0\pi^0$  invariant mass. The differential cross section  $d\sigma/dm_{00}$  is obtained by omitting the  $d\omega$ -integration in eq.(20) and applying the normalization factor  $m_\pi^{-1}\sqrt{\Sigma/s}$ . Fig. 6 shows in percent the radiative corrections to the  $\pi^0\pi^0$  mass spectrum for neutral pion-pair production  $\pi^-\gamma \rightarrow \pi^-\pi^0\pi^0$  as a function of the  $\pi^0\pi^0$  invariant mass  $\sqrt{\Sigma}m_\pi$ . The numbers (4, 5, 6, 7) on the four rising curves correspond to  $\sqrt{s}$ , the total center-of-mass energy divided by  $m_\pi$ . The electromagnetic counterterm  $\bar{k}$  shifts again the whole pattern by a constant  $3\alpha\bar{k}/\pi$ .

In summary, we find that the radiative corrections to neutral pion-pair production  $\pi^-\gamma \rightarrow \pi^-\pi^0\pi^0$  are comparable in size to those for pion Compton scattering  $\pi^-\gamma \rightarrow \pi^-\gamma$  [12].

## References

- [1] G. Colangelo, J. Gasser, H. Leutwyler, *Nucl. Phys.* **B603**, 125 (2001).
- [2] S. Pislak et al., *Phys. Rev.* **D67**, 072004 (2003).
- [3] J.R. Batley et al., *Eur. Phys. J.* **C54**, 411 (2008).
- [4] J.R. Batley et al., *Eur. Phys. J.* **C64**, 589 (2009).
- [5] J. Gasser, M.A. Ivanov, M.E. Sainio, *Nucl. Phys.* **B745**, 84 (2006); and refs. therein.
- [6] Y.M. Antipov et al., *Phys. Lett.* **B121**, 445 (1983); *Z. Phys.* **C26**, 495 (1985).
- [7] J. Ahrens et al., *Eur. Phys. J.* **A23**, 113 (2005).
- [8] R. Garcia-Martin, B. Moussallam, hep-ph/1006.5373.
- [9] COMPASS: P. Abbon et al., *Nucl. Instrum. Meth.* **A577**, 455 (2007); hep-ex/0703049.
- [10] I.Y. Pomeranchuk, I.M. Shmushkevich, *Nucl. Phys.* **23**, 452 (1961).
- [11] N. Kaiser, J.M Friedrich *Eur. Phys. J.* **A36**, 181 (2008).
- [12] N. Kaiser, J.M Friedrich *Nucl. Phys.* **A812**, 186 (2008).
- [13] N. Kaiser, J.M Friedrich *Eur. Phys. J.* **A39**, 71 (2009).
- [14] J. Bijnens, A. Bramon, F. Cornet, *Phys. Lett.* **B237**, 488 (1990);  
J. Bijnens, *Int. J. Mod. Phys.* **A8**, 3045 (1993).
- [15] T. Hannah, *Nucl. Phys.* **B593**, 577 (2001).
- [16] L. Ametller, M. Knecht, P. Talavera, *Phys. Rev.* **D64**, 094009 (2001).
- [17] B. Grube, hep-ex/1020.1272.
- [18] COMPASS collaboration: M.G. Alekseev et al., *Phys. Rev. Lett.* **104**, 241803 (2010).
- [19] N. Kaiser, hep-th/1007.5277.
- [20] M. Knecht, R. Urech, *Nucl. Phys.* **B519**, 329 (1998); and refs. therein.
- [21] J. Gasser, V.E. Lyubovitskij, A. Rusetsky, A. Gall, *Phys. Rev.* **D64**, 016008 (2001).